

A simple but effective approach to generate energy-efficient trajectories of a 2 degree-of-freedom planar manipulator

D. Dona', R. Minto, M. Bottin and G. Rosati

Abstract EU has the ambitious goal of reaching net-zero carbon emissions by 2050. To achieve this, energy savings in the industry can play a relevant role. Considering industrial robots, this paper presents a novel method based on adding a proper law to the base one, which both keeps the robot cycle time-invariant and is easy to implement. In particular, a 2 degree-of-freedom planar manipulator is taken as an example. The method consists of an optimization routine that takes into account the joint speed limit, reducing the energy needed for each movement.

1 Introduction

The reduction of energy expenditure (EE) in robotic systems is a well-known topic [6]. In a typical industrial scenario, motion planning is designed to minimize cycle time to maximize the throughput [3, 2]. At the same time, from both an environmental and an economic point of view, a reduction in EE can be desirable [5]. Various approaches have been proposed over the years to increase efficiency, such as using lighter parts [9, 8], adding elastic elements [11], or using efficient trajectories [4, 10]. The latter has the advantage that no hardware modifications are needed. In addition, efficient trajectories can be used in combination with other approaches, further reducing EE.

In this work, the optimization of a Point-to-Point (PTP) movement of a 2 degrees-of-freedom (DoF) manipulator is analyzed. The procedure is easily extendable to more complex open-chain manipulators and is easy to implement since it relies on simple trajectories and the well-known robot dynamic model [12]. The paper is organized as follows: Sect. 2 presents the mathematical model to be used in the optimization procedure explained in Sect. 3.1; Sect. 4 presents simulated examples; conclusions are drawn in Sect. 5.

D. Dona'
University of Padova, Padua, Italy, e-mail: domenico.dona@phd.unipd.it

2 Mathematical model

Let us consider a 2 DoF planar manipulator with two revolute joints. Referring to Fig. 1, the inverse dynamic model of the manipulator is calculated starting from the Lagrange formulation.

$$\frac{d}{dt} \left(\frac{\delta \mathcal{L}}{\delta \dot{q}} \right) - \frac{\delta \mathcal{L}}{\delta q} = \underline{\tau} \quad , \quad \mathcal{L} = \mathcal{T} - \mathcal{U} \quad (1)$$

where \mathcal{L} is the Lagrangian, q is the vector of the joint variables, \dot{q} is the vector of the joint speeds, $\underline{\tau}$ is the vector of the joint torques, \mathcal{T} is the total kinetic energy, and \mathcal{U} is the total potential energy. Substituting the expression of the kinetic and potential energy into (1) leads us to the following general form for the dynamics of a manipulator:

$$\mathbf{M}(q)\ddot{q} + \mathbf{C}(q, \dot{q})\dot{q} + \mathbf{g}(q) = \underline{\tau} \quad (2)$$

where \mathbf{M} , \mathbf{C} , and \mathbf{g} are inertia, Coriolis matrix, and gravity vector, respectively, and \ddot{q} is the vector of joint accelerations.

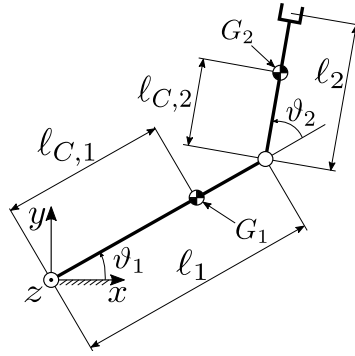


Fig. 1: Model of the 2 DoF manipulator

Let I_{zz_i} be the inertia with respect to the CoM (center of mass) and m_i be the mass of the i -th link, also considering the mass of the motor stator $i+1$. Let $l_{C,i}$ be the distance of the CoM of the i -th link from the i -th joint and l_i me the length of the i -th link. The matrix \mathbf{M} , for the manipulator studied, can be computed as follows:

$$\mathbf{M} = \begin{bmatrix} m_{11} & m_{12} \\ m_{21} & m_{22} \end{bmatrix} \quad (3)$$

Using the notation $\sin_i = \sin \theta_i$ and $\sin_{ij} = \sin(\theta_i + \theta_j)$ (and similarly for the cosine), we have:

$$m_{11} = I_{zz1} + m_1 \ell_{C,1}^2 + k_{r,1}^2 I_{m,1} + I_{zz2} + m_2 \left(\ell_1^2 + \ell_{C,2}^2 + 2\ell_1 \ell_{C,2} \cos_2 \right) + I_{m,2} \quad (4)$$

$$m_{12} = m_{21} = I_{zz2} + m_2 \left(\ell_{C,2}^2 + \ell_1 \ell_{C,2} \cos_2 \right) + k_{r,2} I_{m,2} \quad (5)$$

$$m_{22} = I_{zz2} + m_2 \ell_{C,2}^2 + k_{r,2}^2 I_{m,2} \quad (6)$$

Where $I_{m,i}$ is the inertia of the rotor of the i -th motor. Defining $h = -m_2 \ell_1 \ell_{C,2} \sin_2$ the Coriolis matrix takes the following form:

$$\mathbf{C} = \begin{bmatrix} h\dot{\theta}_2 & h(\dot{\theta}_1 + \dot{\theta}_2) \\ -h\dot{\theta}_1 & 0 \end{bmatrix} \quad (7)$$

The gravity vector $\mathbf{g} = [g_1 \ g_2]^T$ can be computed as:

$$g_1 = (m_1 \ell_{C,1} + m_2 \ell_1) g \cos_1 + m_2 \ell_{C,2} g \cos_{12} \quad (8)$$

$$g_2 = m_2 \ell_{C,2} g \cos_{12} \quad (9)$$

Once the joint torque is calculated with equation (2), it is possible to compute the torque required by the i -th motor by considering the efficiency $\eta_{r,i}$ and the reduction ratio $k_{r,i}$ of the i -th gearbox.

$$\tau_{mot,i} = \frac{\tau_i}{\eta_{r,i} k_{r,i}} \quad (10)$$

2.1 Electrical model

Since most manipulators are driven by DC motors, the electrical subsystem can be described by the electrical model of the DC motor.

The electrical energy E absorbed by the motors from the power grid is the following:

$$E = \sum_{i=1}^N \int_0^{t_f} \mathcal{P}_i(t) dt \quad (11)$$

where N is the number of motors and \mathcal{P}_i is the power absorbed by the i -th motor. Since accumulator capacity is not given, regenerative braking power is dissipated in a braking resistor. From a mathematical point of view, this can be stated as follows.

$$\mathcal{P}_i(t) = \begin{cases} \mathcal{P}_i(t) & \text{if } \mathcal{P}_i(t) > 0 \\ 0 & \text{otherwise} \end{cases} \quad (12)$$

The power delivered at every instant depends on the armature electrical quantities:

$$\mathcal{P}_i(t) = v_{a,i}(t) i_{a,i}(t) \quad (13)$$

Where $v_{a,i}$ and $i_{a,i}$ are the armature voltage and current of the i -th motor, respectively. The voltage armature can be obtained by solving the DC motor equivalent circuit model:

$$v_{a,i}(t) = R_{a,i}i_{a,i}(t) + L_{a,i}\frac{di_{a,i}(t)}{dt} + k_{v,i}k_{r,i}\dot{q}_i \quad (14)$$

Where $R_{a,i}$, $L_{a,i}$, $k_{v,i}$ are the armature resistance, the armature inductance, and the Back EMF constant of the i -th motor, respectively. In the following, the inductive term is neglected under the assumption that the current transients are faster than those of the mechanical subsystem dynamics. Both (13) and (14) depend on the armature current:

$$i_{a,i}(t) = \frac{\tau_{mot,i}(t)}{k_{t,i}} \quad (15)$$

where $\tau_{mot,i}$ is the torque generated by the motor given by (10), and $k_{t,i}$ is the torque constant, numerically equal to $k_{v,i}$.

3 Motion planning algorithm

Hereafter, the subscript i is removed for the sake of brevity; in the following, all the equations are considered to be valid for each joint. The movements of a manipulator are limited by the capability of the motors placed inside the joints. In other words, the movement time T is the maximum of the times needed by all joints when each of them reaches the maximum speed (\dot{q}_{lim}) for a determined motion law. The trajectories of the joints that require less time are scaled to fit T , and thus the maximum joint velocities (\dot{q}_{max}) are reduced. Usually, it is one joint that reaches the limit¹. This means that the other joints have some margin of velocity ($\Delta\dot{q} = |\dot{q}_{lim} - \dot{q}_{max}|$). As a result, we can exploit this difference to modify the base motion law.

Let us consider a PTP task; a common motion law is the symmetrical trapezoidal law of velocity, illustrated in Fig. 2. Given the end joint value and the acceleration time T_a , the law is fully defined.

To exploit the velocity margin, it is introduced a law that has the propriety of having an overall zero displacement, which means that summing it to the base one makes no difference in the final position. In our work, a double trapezoidal law is used. It is composed of two trapezoidal velocity laws, one with positive velocity and the other with negative velocity, as illustrated in Fig. 3. The two periods are defined by the parameter α , which is between 0 and T .

The maximum velocities in the two periods are h_1 and h_2 , respectively. The ratio of acceleration times to the two periods is fixed and equal to t_α .

The additional law is defined by two parameters: h_1 and α ; in fact, h_2 is defined by the condition that Δq of the double trapezoidal law must be zero:

¹ In the case both reach the joint limit no optimization is possible.

$$\int_0^\alpha \dot{q}(t) dt = h_1 \alpha (1 - t_\alpha) = h_2 (1 - t_\alpha) (T - \alpha) = \int_\alpha^T \dot{q}(t) dt \quad (16)$$

$$h_2 = h_1 \frac{\alpha}{T - \alpha}$$

Since joint speed limit \dot{q}_{lim} must not be passed both in positive and negative values, h_1 is constrained as such, based on the maximum joint velocity for the base law \dot{q}_{max} :

$$\begin{aligned} h_1 &\leq \dot{q}_{lim} - \dot{q}_{max} = h_{1,ub} \\ h_1 &\geq -\dot{q}_{lim} - \dot{q}_{max} = h_{1,lb} \end{aligned} \quad (17)$$

The expressions reported in (17) do not consider the possibility of a limit over-taking due to h_2 . The constraints have to be updated through equation (16):

$$h_{1,ub}^*(\alpha) = \min \left[h_{1,ub}, h_{1,ub} \frac{\alpha}{T - \alpha} \right] \quad (18)$$

$$h_{1,lb}^*(\alpha) = \max \left[h_{1,lb}, h_{1,lb} \frac{\alpha}{T - \alpha} \right] \quad (19)$$

The relation between the two bounds and α is nonlinear and not concave.

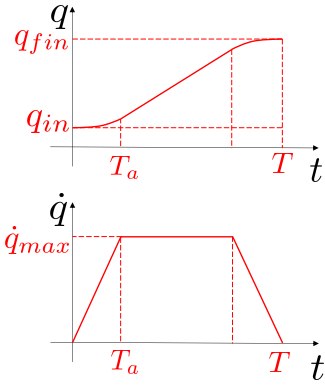


Fig. 2: Symmetrical trapezoidal law of velocity

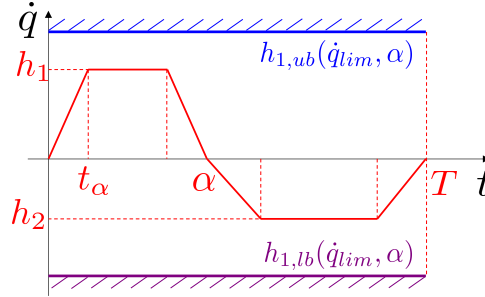


Fig. 3: Double trapezoidal law of velocity

3.1 Optimization procedure

Once the cycle time T is calculated for the bottleneck joint, it is possible to choose α and h_1 for the other joint to minimize energy consumption. Calculating τ_{mot} , and then, by means of equations (14), (15) and (13) it is possible to calculate the

electrical energy absorbed by the motors E (equation (11)). Formally, the following optimization problem must be solved:

$$\begin{aligned} & \underset{\alpha, h_1}{\text{minimize}} && E(\alpha, h_1) && (20) \\ & \text{subject to} && \begin{cases} 0 < \alpha < T \\ h_{1,lb} \leq h_1 \leq h_{1,ub} \end{cases} \end{aligned}$$

Since it is not convex, the global optimality is not ensured by the convergence of the routine [7]. To avoid this problem, several optimization routines with different random starting guesses can be performed.

4 Simulation

To validate our approach, we applied it to a 2 DoF planar manipulator performing a PTP motion; the inertial, electrical, and mechanical properties of the manipulator are listed in Tab. 1. The PTP motion, whose starting and ending positions are reported in Tab. 2, is studied with four different cases (Tab. 3), both with and without gravity and with both configurations (lefty/righty).

Table 1: Model data

	Link 1	Link 2
ℓ [mm]	300	200
I_{zz} [kg·m ²]	0.1	0.1
m [kg]	10	10
ℓ_C [mm]	150	100
I_m [kg·m ²]	$6 \cdot 10^{-7}$	$6 \cdot 10^{-7}$
k_r [l]	120	120
\dot{q}_{lim} [rpm]	4000	4000
k_t [Nm/A]	1.5	1.5
R_a [Ω]	1.5	1.5

Table 2: Initial and final points of the task

Coordinate	Initial P.	Final P.
x [mm]	300	0
y [mm]	0	400

Table 3: Cases studied

Case	Configuration	Gravity
(a)	righty	✓
(b)	righty	✗
(c)	lefty	✓
(d)	lefty	✗

Using the Matlab function `fmincon` and random (but feasible) starting points, the results summarized in Tab. 4 are obtained. The comparison between the reference trajectory and the optimized trajectory is reported in Fig. 4.

Table 4: Optimization results, the energies are expressed in [mJ]

	EE ref.	EE opt.	Δ [%]	h_1 [rad/s]	α [s]
Case (a)	618.4	502.1	19	2.40	0.496
Case (b)	406.8	336.9	17	2.23	0.346
Case (c)	74.3	66.5	11	-4.10	0.478
Case (d)	103.5	100.7	3	-0.79	0.245

In all cases, the introduction of the double trapezoidal law reduces the EE. The savings are from 3% to 19% with a mean of 12.5%, whilst the computational time to calculate the optimal motion law is 89.2s on a Windows PC equipped with an AMD Ryzen 4500U processor and 8 GB of RAM. The cost can be reduced using lower initial guesses (in this case 64 different starting points are used). It is clear that in a practical context, a trade-off between optimality and computational cost has to be evaluated in the design phase. However, it should be noted that, by changing the motion law, the trajectory of the end-effector changes, so collision checks must be performed to ensure the feasibility of the trajectory [1]. The reference and optimal trajectories for each case are shown in Fig. 4.

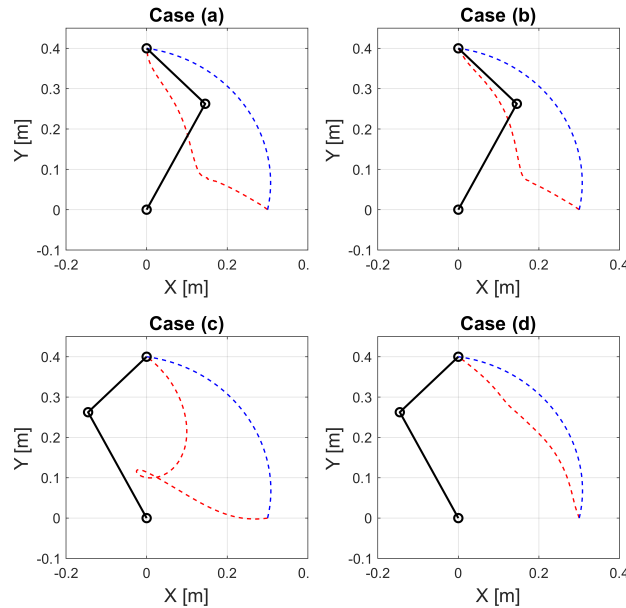


Fig. 4: Comparison of optimal (in red) and reference (in blue) trajectories in the different cases studied. Same starting and final points are used. The left side cases are with gravity (manipulator in the vertical plane) while the right ones are without gravity. The above are in the righty configuration and the below in the lefty one.

5 Conclusions

In this article, a novel optimization method has been presented to achieve energy efficiency in open-chain manipulators, with a particular focus on a 2 DoF planar manipulator. The method, which is based on the electromechanical dynamic model of the manipulator, is based on a modification of a standard motion law to exploit full joint capabilities. In this sense, the movement time is not affected, but it is possible to reduce Energy Expenditure.

Furthermore, this method can be used in more complex robotics systems, since more DoF are added more joints are potential candidates to be optimized.

The method has been implemented in Matlab and four different use cases have been tested. The results show that Energy Expenditure can be reduced by more than 10% with ease.

References

1. Bottin, M., Boschetti, G., Rosati, G.: A novel collision avoidance method for serial robots. *Mechanisms and Machine Science* **66**, 293–301 (2019). DOI 10.1007/978-3-030-00365-4_35
2. Bottin, M., Rosati, G.: Trajectory optimization of a redundant serial robot using cartesian via points and kinematic decoupling. *Robotics* **8**(4) (2019). DOI 10.3390/ROBOTICS8040101
3. Bottin, M., Rosati, G., Boschetti, G.: Working cycle sequence optimization for industrial robots. *Mechanisms and Machine Science* **91**, 228–236 (2021). DOI 10.1007/978-3-030-55807-9_26
4. Brossog, M., Bornschlegl, M., Franke, J., et al.: Reducing the energy consumption of industrial robots in manufacturing systems. *The International Journal of Advanced Manufacturing Technology* **78**(5), 1315–1328 (2015)
5. Carabin, G., Scalera, L., Wongratanaphisan, T., Vidoni, R.: An energy-efficient approach for 3d printing with a linear delta robot equipped with optimal springs. *Robotics and Computer-Integrated Manufacturing* **67**, 102045 (2021). DOI <https://doi.org/10.1016/j.rcim.2020.102045>
6. Carabin, G., Wehrle, E., Vidoni, R.: A review on energy-saving optimization methods for robotic and automatic systems. *Robotics* **6**(4), 39 (2017)
7. Gill, P.E., Murray, W., Wright, M.H.: *Practical optimization*. SIAM (2019)
8. Hagn, U., Nickl, M., Jörg, S., Passig, G., Bahls, T., Nothhelfer, A., Hacker, F., Le-Tien, L., Albu-Schäffer, A., Konietschke, R., et al.: The dlr miro: a versatile lightweight robot for surgical applications. *Industrial Robot: An International Journal* (2008)
9. Kim, Y.J.: Design of low inertia manipulator with high stiffness and strength using tension amplifying mechanisms. In: 2015 IEEE/RSJ International Conference on Intelligent Robots and Systems (IROS), pp. 5850–5856. IEEE (2015)
10. Scalera, L., Boscaroli, P., Carabin, G., Vidoni, R., Gasparetto, A.: Enhancing energy efficiency of a 4-dof parallel robot through task-related analysis. *Machines* **8**(1), 10 (2020)
11. Scalera, L., Carabin, G., Vidoni, R., Wongratanaphisan, T.: Energy efficiency in a 4-dof parallel robot featuring compliant elements. *Int. J. Mech. Control* **20**(02), 49–57 (2019)
12. Siciliano, B., Sciavicco, L., Villani, L., Oriolo, G.: *Robotics: modelling, planning and control*. Springer Science & Business Media (2010)